Cerebello-cortical network fingerprints differ between essential, Parkinson's and mimicked tremors

Muthuraman Muthuraman,[1,*] Jan Raethjen,[2,*] Nabin Koirala,[1] Abdul Rauf Anwar,[2,3] Kidist G. Mideksa,[2,4] Rodger Elble,[5] Sergiu Groppa[1,*] and Günter Deuschl[2,*]

*These authors contributed equally to this work.

Cerebello-thalamo-cortical loops play a major role in the emergence of pathological tremors and voluntary rhythmic movements. It is unclear whether these loops differ anatomically or functionally in different types of tremor. We compared age- and sex-matched groups of patients with Parkinson's disease or essential tremor and healthy controls ($n = 34$ per group). High-density 256-channel EEG and multi-channel EMG from extensor and flexor muscles of both wrists were recorded simultaneously while extending the hands against gravity with the forearms supported. Tremor was thereby recorded from patients, and voluntarily mimicked tremor was recorded from healthy controls. Tomographic maps of EEG-EMG coherence were constructed using a beamformer algorithm coherent source analysis. The direction and strength of information flow between different coherent sources were estimated using time-resolved partial-directed coherence analyses. Tremor severity and motor performance measures were correlated with connection strengths between coherent sources. The topography of oscillatory coherent sources in the cerebellum differed significantly among the three groups, but the cortical sources in the primary sensorimotor region and premotor cortex were not significantly different. The cerebellar and cortical source combinations matched well with known cerebello-thalamo-cortical connections derived from functional MRI resting state analyses according to the Buckner-atlas. The cerebellar sources for Parkinson's tremor and essential tremor mapped primarily to primary sensorimotor cortex, but the cerebellar source for mimicked tremor mapped primarily to premotor cortex. Time-resolved partial-directed coherence analyses revealed activity flow mainly from cerebellum to sensorimotor cortex in Parkinson's tremor and essential tremor and mainly from cerebral cortex to cerebellum in mimicked tremor. EMG oscillation flowed mainly to the cerebellum in mimicked tremor, but oscillation flowed mainly from the cerebellum to EMG in Parkinson's and essential tremor. The topography of cerebellar involvement differed among Parkinson's, essential and mimicked tremors, suggesting different cerebellar mechanisms in tremorogenesis. Indistinguishable areas of sensorimotor cortex and premotor cerebral cortex were involved in all three tremors. Information flow analyses suggest that sensory feedback and cortical efferent copy input to cerebellum are needed to produce mimicked tremor, but tremor in Parkinson's disease and essential tremor do not depend on these mechanisms. Despite the subtle differences in cerebellar source topography, we found no evidence that the cerebellum is the source of oscillation in essential tremor or that the cortico-bulbo-cerebello-thalamocortical loop plays different tremorogenic roles in Parkinson's and essential tremor. Additional studies are needed to decipher the seemingly subtle differences in cerebellocortical function in Parkinson's and essential tremors.

1 Section of Movement Disorders and Neurostimulation, Biomedical Statistics and Multimodal Signal processing unit, Department of Neurology, Focus Program Translational Neuroscience (FTN), University Medical Center of the Johannes Gutenberg-University Mainz, Mainz-55131, Germany
2 Department of Neurology, Christian-Albrechts-University, Kiel-24105, Germany
3 Biomedical Engineering Centre, University of Engineering & Technology, Lahore (KSK Campus)-54890, Pakistan
4 Institute for Circuit and System Theory, Christian-Albrechts-University, Kiel-24143, Germany
5 Department of Neurology, Southern Illinois University School of Medicine, Springfield, 62794-9643, USA

Correspondence to: Prof. Dr.-Ing. M. Muthuraman
Biomedical statistics and multimodal signal processing unit
Movement Disorders and Neurostimulation
Department of Neurology
Focus Program Translational Neuroscience (FTN)
Johannes-Gutenberg-University Hospital
Langenbeckstr. 1
55131 Mainz, Germany
E-mail: mmuthura@uni-mainz.de

Introduction

Tremor is one of the most common and disabling movement disorders (Zeuner and Deuschl, 2012). It is defined as an involuntary oscillatory movement. Different forms of tremor have been described. Symptomatic physiological tremor may occur in healthy individuals (Gross *et al.*, 2002), while debilitating tremor occurs in neurological disorders such as Parkinson's disease, essential tremor and dystonia. The hallmark of Parkinson's disease is rest tremor, but action tremor is also common. Upper extremity action tremor is characteristic of essential tremor.

A pathophysiological hallmark of tremor is oscillation in the cortico-bulbo-cerebello-thalamo-cortical loop. The components of this loop have been revealed by coherent source analysis of tremor-related activity and mainly include cerebellum, thalamus, motor cortex, and premotor cortex (PMC) (Timmermann *et al.*, 2003; Schnitzler *et al.*, 2009). The cortico-bulbo-cerebello-thalamo-cortical loop is involved in essential tremor, Parkinson's tremor and mimicked tremor in healthy subjects (Muthuraman *et al.*, 2012). A pressing question is if and how the pathophysiology of this loop differs among the many different forms of tremor. We recently found unidirectional connectivity flow in the thalamo-cortical pathway during voluntary rhythmic movement, as opposed to bidirectional exchange in Parkinson's tremor and essential tremor (Muthuraman *et al.*, 2012). Thus, a bidirectional oscillatory loop-type of interaction appears to be an important mechanism in pathological tremors (Muthuraman *et al.*, 2012). In Parkinson's disease, oscillation in the basal ganglia appears to trigger oscillation in the cerebello-thalamo-cortical pathway (Helmich *et al.*, 2012), but the cerebellum is hypothesized to be the primary or triggering source of oscillation in essential tremor. It is noteworthy that voluntary rhythmic hand movements can be performed in the presence of involuntary tremors in essential tremor and Parkinson's disease (Costa *et al.*, 2010). Simultaneous voluntary and involuntary oscillations (tremor) are likely to emerge from shared but different anatomical and functional connections in the same cortico-bulbo-cerebello-thalamo-cortical loop. To test this hypothesis, we used high resolution EEG recordings for coherent source analysis to show, for the first time, that anatomically distinct areas of the cerebellum are activated in essential tremor, Parkinson's tremor and mimicked tremor.

Materials and methods

Subjects

Thirty-four patients with definite Parkinson's disease, as diagnosed by the London Brain Bank criteria (Hughes *et al.*, 1992), participated after giving their informed written consent. Thirty-four patients with essential tremor were diagnosed according to the 1998 diagnostic criteria of the Movement Disorder Society (Deuschl *et al.*, 1998). Thirty-four age- and sex-matched volunteers with normal neurological exams constituted a control group. The demographics of these groups are shown in Table 1.

Participants were seated in a comfortable chair in a slightly reclined position. Both forearms were supported to the wrists by firm armrests. The first recording was a resting state of 10 min with eyes closed. In the second recording, the hands were held outstretched against gravity, and the participants were asked to keep their eyes open and fixed on a point ~2 m away. Parkinson's disease patients with rest tremor that persisted during posture at similar frequency were selected. In this study we have only analysed the postural tremor in Parkinson's disease patients. No participant had impaired cognitive function on clinical exam, and their medications were not changed for this study. The Mini-Mental State Examination cognitive scores are included in Table 1. Medications for the Parkinson's disease and essential tremor patients are listed in Supplementary Table 1.

Tremor was recorded with surface EMG from the forearm flexors and extensors using silver-silver chloride electrodes. EEG was recorded simultaneously with a high-resolution 256-channel recording system (EGI, www.egi.com), with CZ as reference. Data were stored in a computer and analysed off-line. Individual recordings were of 2 min duration. The number of recordings performed on each person varied between one and three, depending on the person's tolerance of the experimental procedure.

All healthy subjects were asked to perform rhythmic extension-flexion wrist movements as fast as possible for 2 min to mimic hand tremor. The healthy subjects were asked to produce the rhythmic movements in a self-paced manner. The

Table 1 Demographics and spectral values

Parameters	Parkinson's disease	Essential tremor	Controls
n	34	34	34
Male/female	25/9	25/9	25/9
Mean age	59.7 ± 9	58.9 ± 9	58 ± 9
Disease duration	22 ± 15	21 ± 16	–
Tremor frequency	4.49 ± 0.75	5.12 ± 1.12	4.56 ± 1.23
EEG-SNR (dB)	21.24 ± 2.26	20.26 ± 3.09	21.54 ± 1.96
EMG-SNR (dB)	31.47 ± 4.65	32.56 ± 3.89	31.56 ± 3.09
EMG total power 2–40 Hz (log)	4.64 ± 1.78	4.98 ± 1.90	4.94 ± 3.87
Cognitive MMSE score	27.04 ± 1.31	28.23 ± 1.05	29.32 ± 0.85

MMSE = Mini-Mental State Examination; SNR = signal-to-noise ratio.

consistency of rhythmic movements was monitored for each subject by analysing the EMG activity online, and a frequency of at least two to five bursts per second was required. The time windows with lower frequencies were discarded. Sixteen controls could not sustain the movements for more than 1 min and therefore performed the task twice.

Data preprocessing

The methods used in this study are illustrated schematically in Fig. 1. EEG and EMG were sampled at 1000 Hz and band-pass filtered (EMG 30–200 Hz; EEG 0.05–200 Hz). EMG was full-wave rectified before filtering, producing demodulated EMG (Journee, 2007). Each recording was segmented into a number of 1-s epochs (L = 1000), discarding all data segments with visible artefacts. Depending on the length (N) of the recording and the quality of the data, 220–240 1-s epochs (M) were used for analysis, such that N = LM. The signal-to-noise (SNR) ratio was estimated by dividing the spectral power at 2–7 Hz by the power in the 300–400 Hz band (considered as background noise for the EEG and EMG).

Coherence analysis

The coherence spectrum was estimated using the Welch periodogram method (Welch, 1967). The statistical significance (Halliday *et al.*, 1995) of the coherence at a particular frequency is calculated by:

$$1 - (1 - \chi)^{1/(M-1)} \quad (1)$$

Where χ is set to 0.99, so that the confidence limit is $1 - 0.01^{1/(M-1)}$ Values of coherence above this confidence limit are considered to indicate statistically significant linear correlation between the two time series, while values below this limit indicate the absence of correlation. Our next step was to analyse the dynamics of these frequency oscillations over time by applying the multitaper method for each recording (Muthuraman *et al.*, 2010*a*).

Time–frequency analysis

The dynamics of signals in the time and frequency domains were computed with the multitaper method (Mitra and Pesaran, 1999). In this method, the spectrum is estimated by multiplying the data $x(t)$ with K different windows (i.e. tapers). The complete description of the method is explained elsewhere (Muthuraman *et al.*, 2010*a*). The time step was 50 ms with overlapping windows of 1000 ms, providing an approximate time resolution of 50 ms and an approximate frequency resolution of 1 Hz. In a further analysis, all initial coherence estimates of the individual EEG electrodes were combined to get a pooled coherence estimate. This can be done by computing the individual second-order spectra using a weighting scheme and estimate the coherence to obtain the pooled estimate of the individual EEG electrodes (Rosenberg *et al.*, 1989; Amjad *et al.*, 1997). From the pooled time–frequency spectrum, the time intervals with significant coherence between the EEG and EMG at the tremor frequency were selected for all the patients and healthy controls.

Source analysis

Dynamic imaging of coherent sources was used to localize brain activity that was coherent with the peripheral EMG signal (Gross *et al.*, 2001). To locate the origin of a specific EEG activity seen on the scalp, the forward and the inverse problems had to be solved.

The forward problem is the computation of the scalp potentials for a set of neural current sources. It is usually solved by estimating the lead-field matrix with specified models for the brain; a finite-element method is used (Wolters *et al.*, 2007). For the forward modelling, the surfaces of the compartments like the scalp, skull, and brain were extracted from the individual T_1 MRI, and the individual electrode locations obtained from a Polhemus system were used.

The inverse problem is finding the relation between the underlying neural activities and the electric potentials recorded on the scalp. This can be solved by a linear transformation using a spatial filter (van Veen *et al.*, 2002). The spatial filter attenuates the signals from other locations and allows signals generated from a particular location in the brain, for a certain frequency band. The detailed description of the forward and inverse solutions is provided elsewhere (Muthuraman *et al.*, 2008, 2010*b*).

Dynamic imaging of coherent sources is a beamforming technique (Sekihara and Scholz, 1996; Gross and Ioannides, 1999) that uses a spatial filter (van Veen *et al.*, 2002) to compute tomographic maps of cerebro-muscular coherence in the frequency band of interest. Source analysis was restricted to cortical, immediate subcortical and cerebellar voxels because these regions were directly under the high density electrode array of

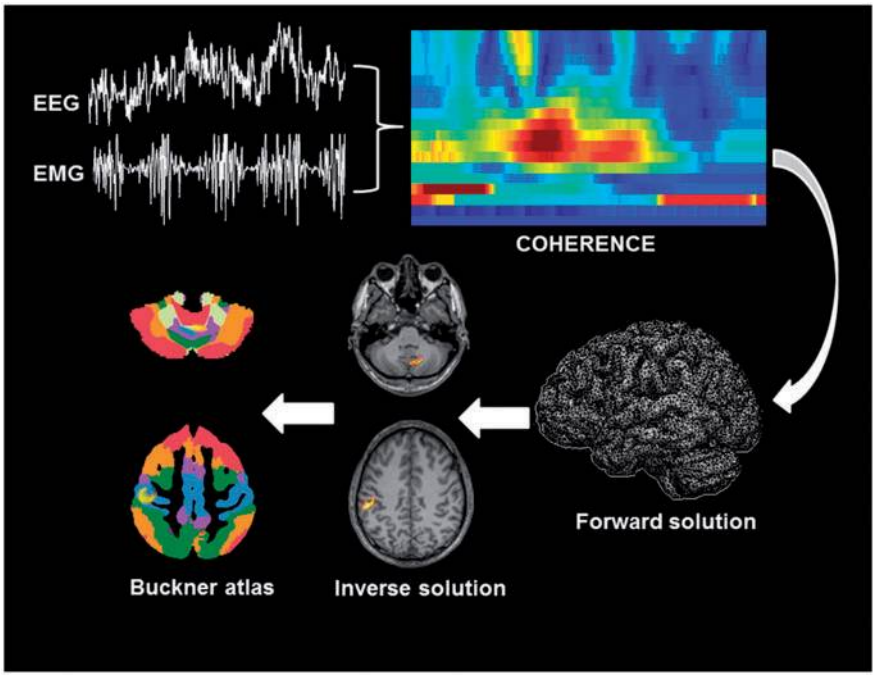

Figure 1 The pipeline used in this study is shown schematically with a representative figure for each step. The raw EEG and EMG data after preprocessing are subjected to time–frequency analyses to estimate the coherence and to select the time intervals with high coherence. The third step is the forward solution, producing a realistic head model for each subject. The fourth step is the inverse solution to identify the network of sources at the tremor or mimicked tremor frequency. The final step is to interpolate the identified cerebellar and cortical sources on the coloured Buckner atlas (Buckner *et al.*, 2011).

the EEG cap, yielding high signal-to-noise ratios and most reliable source identification and location. The spatial filter was applied to a large number of voxels in these regions, assigning to each voxel a specific value of coherence to a given reference signal. A voxel size of 2 mm was used in this study. The source in the regions of interest with the strongest coherence to the EMG signal at the tremor frequency was identified. Since the coherence between the identified areas with itself is always 1, this region was projected out of the coherence matrix, and additional coherent areas were identified (Gross *et al.*, 2002). Once coherent cerebral cortical and cerebellar areas were identified, their activity was extracted by the spatial filter (van Veen *et al.*, 2002). The individual maps of the strongest cerebro-muscular coherence were spatially normalized, averaged and displayed on a standard Montreal Neurological Institute (MNI) template brain in statistical parametric mapping (SPM8). We also constructed a grid for each individual subject in such a way that these grids are aligned to that of the MNI space, in order to take into account the individual anatomical differences between the subjects. Local maxima in the resulting maps represent areas that have the strongest coherence to the EMG signal. Identified sources were projected to templates of the cerebellum and cerebral cortex from Buckner *et al.* (2011), which colour code the different functional cerebellocortical connections as defined by correlated resting state functional MRI activity. This atlas gives us the corresponding cerebral cortical functional connectivity information for seven cerebellar seed regions. For the cortical and cerebellar sources, the MNI coordinates were extracted from the peak voxel in the identified coherent tomographic maps. The Euclidean distance was estimated between the identified peak voxels in the cerebral cortical and cerebellar sources, and coordinates from the Buckner atlas were used as the reference. To demonstrate the actual spatial resolution achieved by the methods applied in this study for the identified sources in sensorimotor cortex (SMC), PMC and cerebellum, we estimated the Euclidean distances among the 34 subjects in each cohort ($34 \times 33 = 1122$ combinations for each source) for each of three sources separately by taking the MNI coordinate of the maximum coherent voxel (Supplementary material).

Connectivity analyses

Using time–frequency causality, we can focus on a particular frequency and can also analyse the dynamics of the causality at that frequency. The time–frequency causality estimation method of temporal partial directed coherence (TPDC) is based on dual-extended Kalman filtering (Haykin, 2001; Wan and Nelson, 2001) and allows time-dependent autoregressive coefficients to be estimated. One extended Kalman filter estimates the states and feeds this information to a second extended Kalman filter that estimates the model parameters and shares this information with the first. By using two Kalman filters in parallel, we estimated the states and model parameters of the system at each time instant. Time-dependent multivariate coefficients were used in the calculation of causality between the time series. By calculating the time-dependent multivariate autoregressive coefficients at each time point, we also calculated partial directed coherence at each time point. The frequency bands used were the frequencies of the pathological and mimicked tremors. After estimating the TPDC values, the significance level was calculated from

the applied data using a bootstrapping method (Kaminski *et al.*, 2001). In short, we divided the original time series into smaller non-overlapping windows and randomly shuffled the order of these windows to create a new time series. A multivariate autoregressive model was fitted to the shuffled time series, and TPDC was estimated. The shuffling process was done 1000 times, and the average TPDC value was taken as the significance threshold for all connections. This process was performed separately for each patient. The resulting value was the significance threshold value for all connections. The open source MATLAB package autoregressive fit (ARFIT) (Neumaier and Schneider, 2001; Schneider and Neumaier, 2001) was used for estimating the autoregressive coefficients from the spatially filtered source signals. We applied time reversal technique (Haufe *et al.*, 2013) as a second significance test on the connections already identified by TPDC using data-driven bootstrapping surrogate significance test.

Statistical analysis

The total data lengths among the subjects were tested using a non-parametric Friedman test for independent samples ($n = 34$, $P = 0.01$). The interindividual differences in the source locations within each group of subjects ($n = 34$, $P = 0.01$) were tested using a non-parametric Kruskal-Wallis test. The Euclidean distance within the subjects was tested using a non-parametric Kruskal-Wallis test. The statistical significance of the sources ($n = 34$, $P = 0.01$) was tested by a within-subject surrogate analysis. A Monte-Carlo test of 100 random permutations was carried out, and the *P*-values were calculated (Maris and Oostenveld, 2007; Maris *et al.*, 2007). The *P*-value for each of these 100 random permutations was estimated, and then the 99th percentile *P*-value was taken as the significance level for each subject (Moeller *et al.*, 2013). A 1200 ms block length was chosen by an adaptive block length selection method (Mader *et al.*, 2013). We checked for medication effects on our findings by including medication as a covariate in all the statistical analyses, and we did not find any significant correlations between medications and the estimated connectivity parameters. The TPDC values ($n = 34$, $\alpha = 0.01$) between the source signals were tested for significance using a multifactorial ANOVA, within-subject factors being the interactions of the source signals to the cerebellum and vice versa ($n = 4$ Parkinson's disease, $n = 4$ essential tremor, $n = 4$ controls) and the between-subject factor being the diagnosis ($n = 3$ Parkinson's disease, essential tremor, controls). The TPDC values ($n = 34$, $\alpha = 0.01$) between the source signals and EMG were tested for significance using a multifactorial ANOVA, within-subject factors being the interactions of the source signals with the EMG and vice versa ($n = 6$ Parkinson's disease, $n = 6$ essential tremor, $n = 6$ controls) and the between-subject factor being the diagnosis ($n = 3$ Parkinson's disease, essential tremor, controls). Pearson correlation coefficients were estimated and evaluated separately for TPDC values versus the sum of Unified Parkinson's Disease rating Scale (UPDRS)-III items 20 and 21 in Parkinson's disease, a Fahn-Tolosa-Marin subscore (Section A: items 5, 6 and Section B: items 11, 12, 13) in essential tremor, and EMG amplitude in controls. A Bonferroni correction was performed for all the *post hoc* tests that involved multiple comparisons and considered significant at $P < 0.01$.

Results

EEG-EMG coherence and their dynamics over time

Data lengths were not significantly different among the three groups ($P > 0.3$). Power spectral analysis of the EMG activity for all three tremors revealed a dominant peak at the basic tremor frequency, which ranged from 2 to 7 Hz (Table 1). In this frequency band, all subjects exhibited significant coherence between the EMG and EEG electrodes over the region of the contralateral sensorimotor cortex. The time intervals with the highest pooled significant cortico-muscular coherences were used for source analyses.

Coherent cerebellar and cortical sources

The spatial activation in the cerebellum of Parkinson's disease patients is shown in Fig. 2. The applied source analysis identified cerebral cortical sources in the region of the SMC, PMC, supplementary motor area, and posterior parietal cortex. In patients with essential tremor, the spatial activation in the cerebellum was located slightly more anteriorly and laterally than in Parkinson's disease (Fig. 2). The cerebral cortical sources in essential tremor were similar to the cortical sources in Parkinson's disease (Fig. 2). In healthy subjects, the spatial activation in the cerebellum was located more laterally and posteriorly than in the other two groups (Fig. 2). The cerebral cortical sources extracted from healthy subjects were similar to the cortical sources in Parkinson's disease and essential tremor (Fig. 2).

The source coherence values for SMC, PMC and cerebellum did not differ statistically among the three groups (Supplementary Tables 2 and 3). The Euclidian distances between the cerebellar sources differed statistically among essential tremor, Parkinson's disease and controls (Supplementary Table 4). By contrast, the Euclidean distances between the sensorimotor cortical sources did not differ statistically among groups (Parkinson's disease versus essential tremor: $t = 1.45$; $P = 0.58$; essential tremor versus controls: $t = 1.69$; $P = 0.46$; Parkinson's disease versus controls: $t = 1.83$; $P = 0.39$). All of the identified sources within each group of subjects were statistically significant ($t = 4.69$; $P = 0.001$; $t = 4.28$; $P = 0.004$; $t = 3.84$; $P = 0.007$). The spatial resolution for cerebral cortical sources was estimated to be 2–4 mm, and the estimated spatial resolution for cerebellar sources was 4–6 mm (Supplementary material).

Relation to well-known functional cerebellocortical connections

In Fig. 3, the cerebellar and cerebral cortical sources are superimposed on the colour-coded maps of the different cerebellocortical connections, described by Buckner *et al.* (2011). The cerebellar sources for essential tremor and

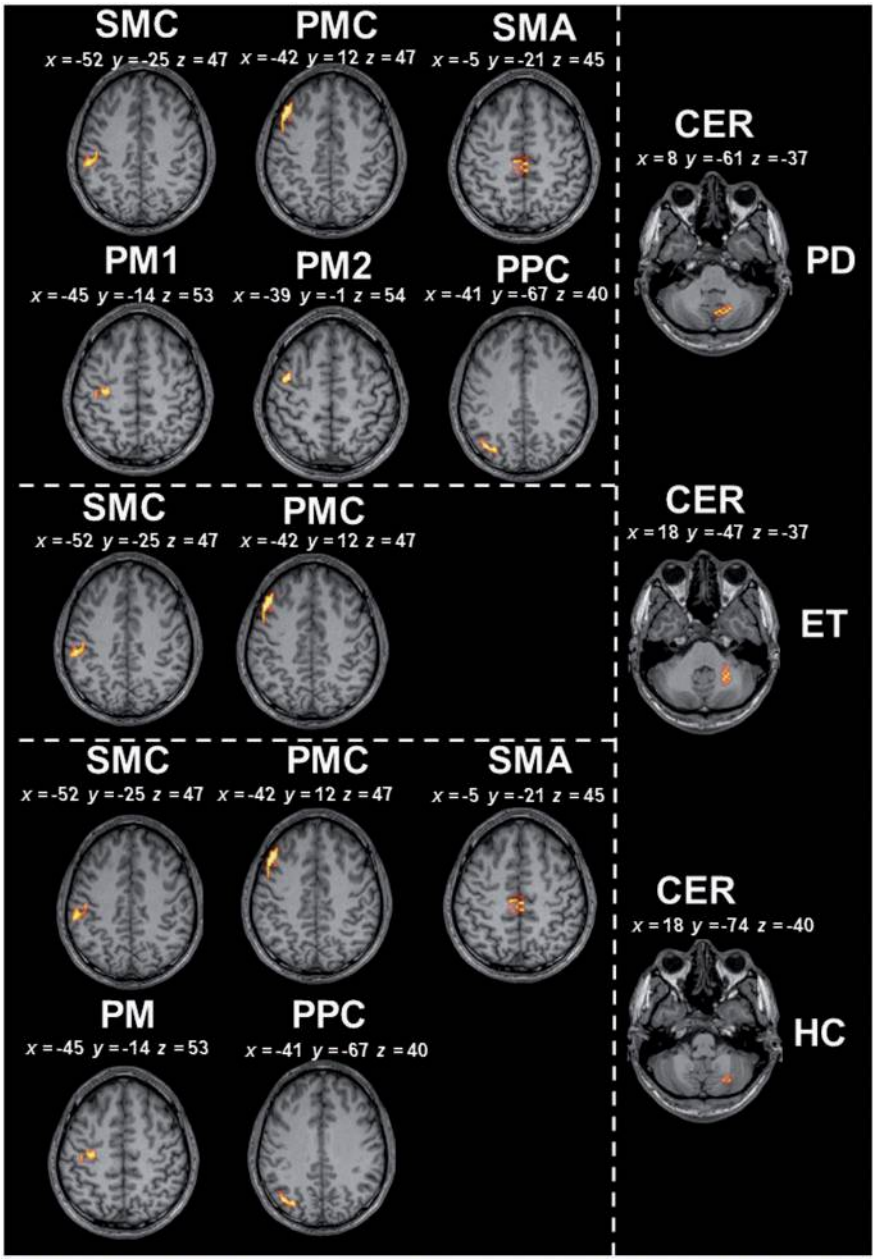

Figure 2 Cerebral cortical and cerebellar sources. The *top* two rows contain the topographic representation of all cerebral cortical and cerebellar sources for Parkinson's disease in an individual T_1 template constructed from all 34 patients. The *middle* row contains the topographic representation of all cerebral cortical and cerebellar sources for essential tremor in an individual T_1 template constructed from all 34 patients. The *bottom* two rows contain the topographic representation of all cerebral cortical and cerebellar sources for controls in an individual T_1 template constructed from all the 34 controls. CER = cerebellum; ET = essential tremor; HC = healthy controls; PD = Parkinson disease; SMA = supplementary motor area.

Parkinson's disease mapped to SMC (Fig. 3, blue), whereas the cerebellar source for mimicked tremor mapped to premotor cortex (Fig. 3, green).

Effective connectivity between cerebellar and cortical sources

We examined interactions between source signals in SMC, PMC and cerebellum at the tremor frequency and between these sources and EMG. In the within-group statistics, only significant differences will be discussed. The TPDC values for the cerebellum to SMC interaction was significantly higher ($t = 5.98$, $P = 0.0006$; $t = 6.06$, $P = 0.0004$) than for the opposite direction in both essential tremor and Parkinson's disease, but in the healthy subjects, the interaction from SMC to cerebellum was significantly higher ($t = 6.10$, $P = 0.0003$) than for the opposite direction. The TPDC values for the direction from PMC to cerebellum

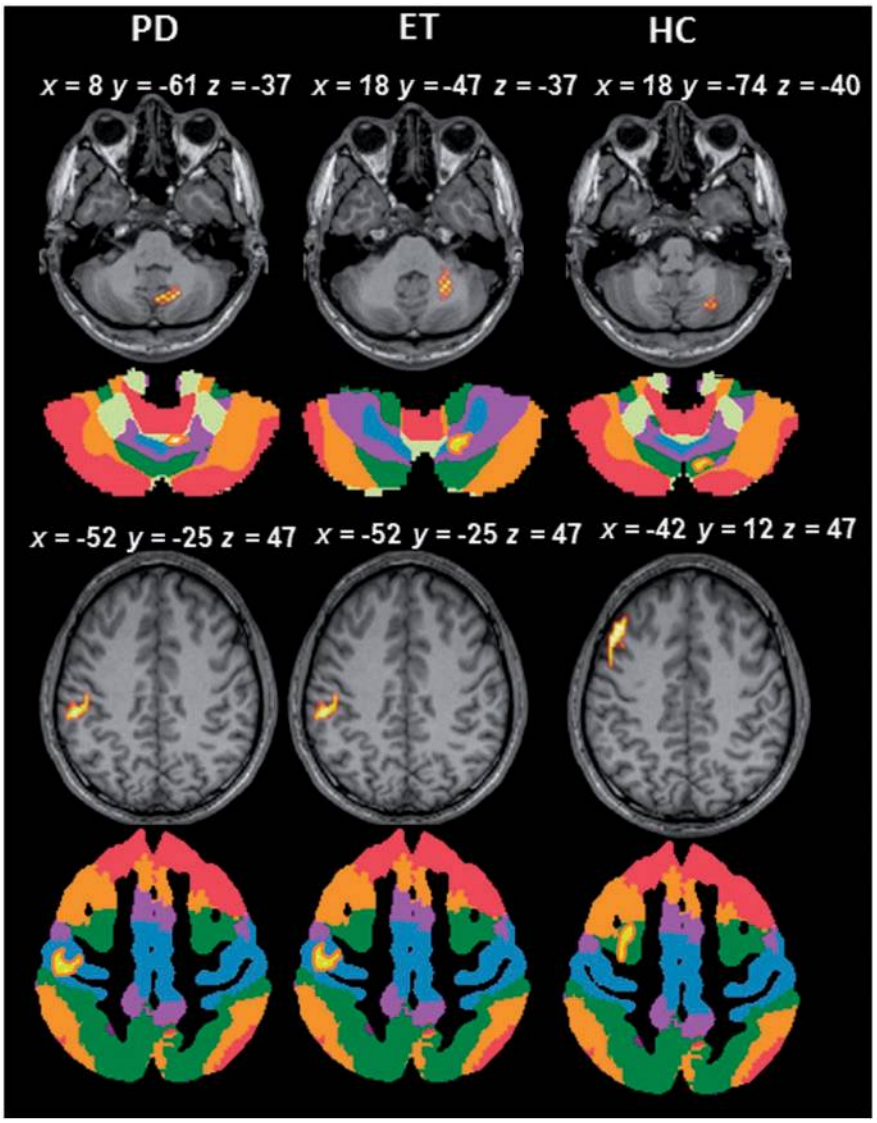

Figure 3 Distinctive cerebellar sources and their corresponding cortical connections. The first row contains the topographic representation of cerebellum for all Parkinson's disease patients (first column), patients with essential tremor (second column) and healthy controls (third column) in an individual T_1 MNI template constructed from the 34 subjects in each group. The second row is the interpolation on the Buckner atlas. The third row is the grand average of the primary sensorimotor cortex sources for Parkinson's disease and essential tremor and the premotor source for controls, interpolated on an individual T_1 MNI template. The last row contains the corresponding primary sensorimotor cortex and premotor cortex interpolated on the Buckner atlas (Buckner *et al.*, 2011). ET = essential tremor; HC = healthy controls; PD = Parkinson disease.

interaction was significantly higher in healthy subjects ($t = 5.92$, $P = 0.0006$; $t = 6.02$, $P = 0.0004$) compared to both essential tremor and Parkinson's disease, and the interaction from PMC to cerebellum in healthy subjects was significantly stronger ($t = 6.21$, $P = 0.0003$) than for the opposite direction. The results are shown as bar graphs in Fig. 4.

The TPDC values for the interaction from the SMC to EMG was significantly higher ($t = 5.82$, $P = 0.0008$; $t = 5.71$, $P = 0.0009$; $t = 6.32$, $P = 0.0002$) than for the opposite direction in all three groups. The information flow for PMC to EMG was significantly higher ($t = 4.37$, $P = 0.008$) than for the EMG to PMC in healthy subjects only. The most striking difference was that the interaction from cerebellum to EMG was significantly higher than EMG to cerebellum in Parkinson's disease and essential tremor ($t = 6.18$, $P = 0.0003$; $t = 5.98$, $P = 0.0007$), but the opposite was true in healthy controls ($t = 4.78$, $P = 0.002$). These results are illustrated in Fig. 5.

We also found that the interaction from SMC to cerebellum was significantly higher in healthy controls compared to essential tremor and Parkinson's disease ($t = 6.02$, $P = 0.0006$; $t = 6.13$, $P = 0.0004$). Interaction from cerebellum to SMC was significantly higher in essential tremor and Parkinson's disease than in healthy controls ($t = 6.17$, $P = 0.0003$; $t = 6.29$, $P = 0.002$). For the

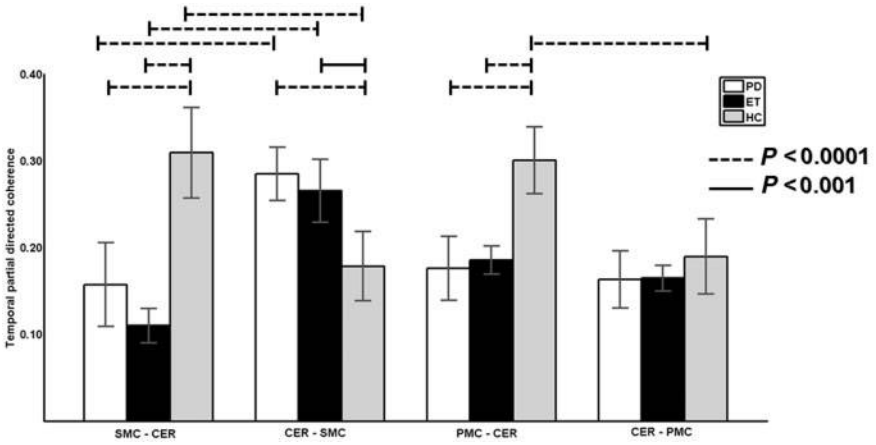

Figure 4 Connectivity from cerebellum to motor cortex. The mean and standard deviation of TPDC values are shown for the connections from cerebellum (CER) to SMC and PMC at the tremor frequency for Parkinson patients (PD), essential tremor patients (ET) and healthy controls (HC; mimicked tremor). All bars shown in the figure are significant connections. The significantly different connections between each pair of sources are marked with either dashed lines for $P < 0.0001$ or bold lines for $P < 0.001$.

connection PMC to cerebellum, the healthy controls had higher information flow compared to Parkinson's disease and essential tremor ($t = 6.09$, $P = 0.0005$; $t = 6.85$, $P = 0.0001$).

For the connection SMC to EMG, we found higher information flow in healthy controls than in Parkinson's disease ($t = 4.65$, $P = 0.003$) and essential tremor ($t = 6.75$, $P = 0.0002$), and Parkinson's disease was significantly higher than essential tremor ($t = 6.04$, $P = 0.0006$). The direction from EMG to PMC was significantly higher for Parkinson's disease ($t = 6.24$, $P = 0.0005$) and essential tremor ($t = 6.68$, $P = 0.0003$) compared to healthy controls. In the direction cerebellum to EMG, the Parkinson's disease patients had significantly higher information flow than patients with essential tremor ($t = 4.79$, $P = 0.004$) and controls ($t = 4.59$, $P = 0.007$). However, the information flow from EMG to cerebellum was significantly stronger for the healthy controls compared to Parkinson's disease ($t = 6.72$, $P = 0.0002$) and essential tremor ($t = 6.97$, $P = 0.0001$), and information flow was significantly higher in Parkinson's disease ($t = 6.22$, $P = 0.0004$) than essential tremor.

We found a significant positive correlation between the cerebellum-to-SMC connection strength (TPDC value) and the UPDRS-III scores (items 20 and 21) in Parkinson's disease (r = 0.4847; $P = 0.0037$) and the Fahn-Tolosa-Marin scores (Section A: items 5, 6 and Section B: items 11, 12, 13) in essential tremor (r = 0.5219; $P = 0.0015$). For healthy controls, we found a significant positive correlation between the PMC-to-cerebellum connection and EMG amplitude of the mimicked tremor (r = 0.4449; $P = 0.0084$). The regression lines are shown in Fig. 6. The other correlations between the connectivity values and tremor frequency or EMG amplitude were not significant.

Discussion

Using high definition EEG, we found different coherent sources in the cerebellum for Parkinson's tremor, essential tremor, and mimicked tremor. These cerebellar sources mapped to motor cortex in essential tremor and Parkinson's disease and to premotor cortex in controls. Flow of oscillatory activity was primarily from cerebellum to cerebral cortex and EMG in essential tremor and Parkinson's disease but activity flow was in the opposite directions in controls. Our results were validated by significant correlations between measures of tremor severity and the strengths of interaction in cerebellocortical connections.

Other imaging and electrophysiological studies have shown that the cerebellum is a key structure in the emergence of essential and Parkinson's tremors (Jenkins *et al.*, 1993; Bucher *et al.*, 1997; Timmermann *et al.*, 2003; Newman, 2006; Helmich *et al.*, 2012; Muthuraman *et al.*, 2012), and Parkinson's and essential tremors can be reduced to a similar extent by high frequency stimulation of the cerebellar receiving nucleus in the ventrolateral thalamus (Fasano and Deuschl, 2015). The cerebellum is also important for the control of repetitive voluntary movements (Salvador *et al.*, 2005). Our data show that the cerebellum is not only an important component of the tremor networks but that the topography of cerebellar activity differs among essential tremor, Parkinson's disease and controls. Nevertheless, all three sources mapped to regions of the cerebellum that connect with motor cortex (essential tremor and Parkinson's disease) or premotor cortex (controls), and these cerebellar regions are known to connect with the interposed nuclei (Benagiano *et al.*, 2018). The interposed nuclei receive abundant somatosensory feedback from the periphery and are known to be involved in animal models of cerebellar tremor (Elble *et al.*, 1984;

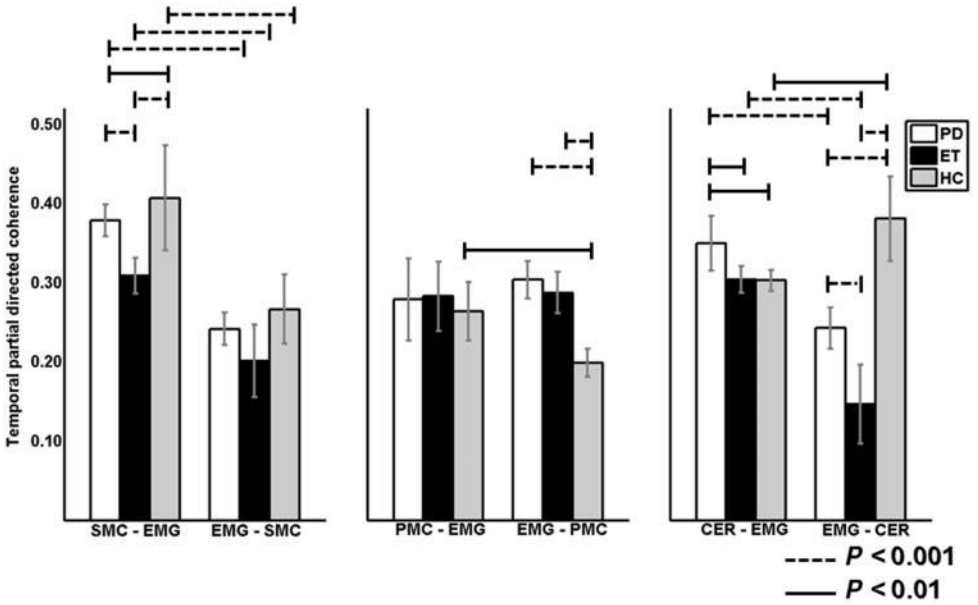

Figure 5 Connectivity from motor cortex and cerebellum to the periphery. The mean and standard deviation of TPDC values for the connections from cerebellum (CER), SMC and PMC to the periphery (EMG) at the tremor frequency for Parkinson's disease patients (PD), essential tremor patients (ET) and healthy controls (controls; mimicked tremor). All bars in the figure are significant connections. The significantly different connections between each pair of sources are marked with either dashed lines for $P < 0.001$ or bold lines for $P < 0.01$.

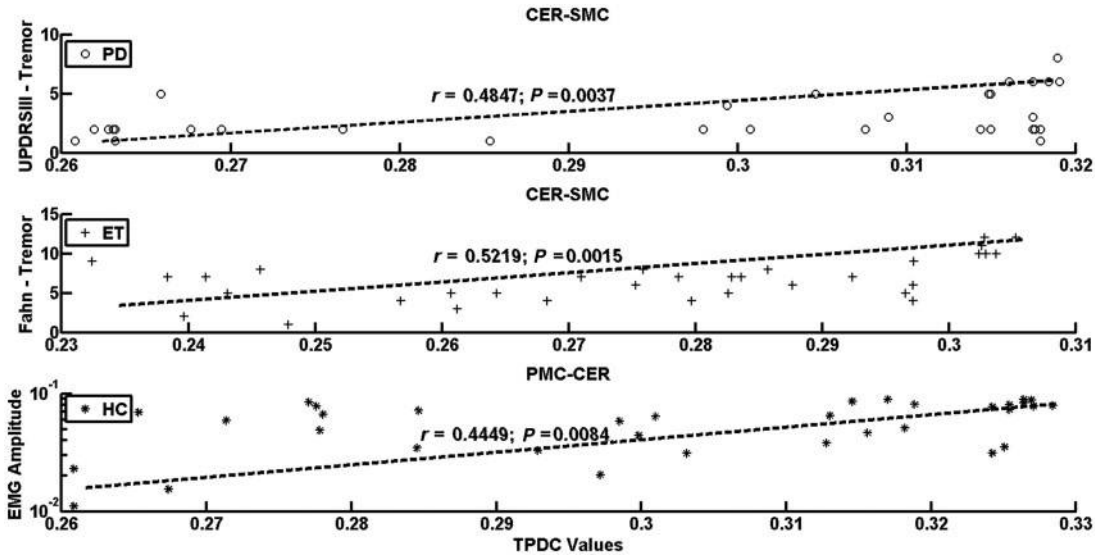

Figure 6 Correlation between specific connections and clinical scores. Linear regression lines are shown for the UPDRS-III score (items 20 and 21) versus mean TPDC values for the connection cerebellum to SMC in Parkinson's disease (*top* graph), Fahn-Tolosa-Marin score (Section A: items 5, 6 and Section B: items 11, 12 and 13) versus mean TDPC values for the connection cerebellum to SMC in essential tremor (*middle* graph), and EMG amplitude of the rhythmic movement versus mean TDPC values for the connection PMC to cerebellum in controls (*bottom* graph). CER = cerebellum; ET = essential tremor; HC = healthy controls; PD = Parkinson disease.

Manto, 2009). The cerebellar source in control subjects is more posterior than in Parkinson's disease and essential tremor sources, so some signal may be coming from areas of cerebellum that connect with dentate (see Fig. 5 in Benagiano *et al.*, 2018). This seems likely because mimicked tremor in controls is a voluntary movement that probably requires efferent copy and motor planning via cortico-bulbo-cerebellar pathways, consistent with the predominant flow of activity from cortex to cerebellum in our study.

Similar regions of cerebral cortex were activated in essential tremor, Parkinson's disease and controls. We previously

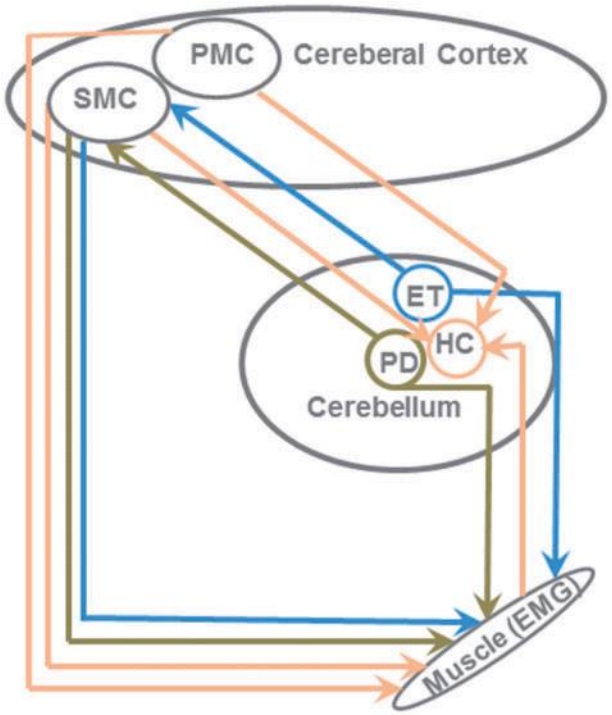

Figure 7 Information flow between the cortico-cereberal sources and the periphery. A representative figure showing the directions of information flow among the cerebellum, cerebral cortex and muscle in Parkinson's disease, essential tremor and controls. PD = Parkinson disease; ET = essential tremor; HC = healthy controls.

reported unidirectional connectivity flow in the thalamo-cortical pathway during voluntary rhythmic movement, as opposed to bidirectional exchange in Parkinson's tremor and essential tremor (Muthuraman *et al.*, 2012). Thus, a bidirectional oscillatory loop-type of interaction may be an important mechanism in pathological tremors (Muthuraman *et al.*, 2012). These cortical areas provide strong excitatory feedback to their thalamic projection sites, which could further enhance tremorogenic oscillation (Ilinsky and Kultas-Ilinsky, 2002).

The cerebellar source in essential tremor was most anterior and was clearly in the motor cerebellum, as previously shown by Broersma and co-workers (2015). Therefore, one would expect that essential tremor is dominated by the interposed nuclei. The cerebellar source in Parkinson's disease seems to fall between essential tremor and controls, but the functional MRI study of Dirkx and colleagues (2017) found anterior lobe involvement in Parkinson's disease also. The work of Helmich and co-workers suggests that the initial path to cerebellar involvement in Parkinson's disease is pallidum-thalamus-cerebral cortex-pontine nuclei-cerebellum (Helmich *et al.*, 2011; Dirkx *et al.*, 2017). Projections to dentate and the lateral cerebellum may be involved in the initial spread of oscillation from basal ganglia to the thalamus (Supplementary Fig. 1) and then to the cortico-bulbo-cerebello (dentato)-thalamocortical loop, but sustained tremor may be mediated primarily by the interposed pathway. Our results for Parkinson's disease and essential tremor were similar and suggest that the cortico-bulbo-cerebello (interposito)-thalamocortical loop plays a pivotal role in sustaining tremor in Parkinson's disease and essential tremor. Our data provide no support for the hypothesis that essential tremor is primarily a cerebellar disorder, compared to tremor in Parkinson's disease. Although the cerebrum is similarly involved in both pathological tremors, the cerebello-cortical channels (Buckner *et al.*, 2011) seem to differ and may be one central basis for the clinical and pathophysiological differences.

The cerebellar sources were not in the lateral cerebellar cortex, which connects with the dentate. The dentate does not receive somatosensory feedback from the periphery (Benagiano *et al.*, 2018). Part of the dentate is 'motor', but another part is 'nonmotor' (Benagiano *et al.*, 2018). In one primate model of tremor, the interposed nuclei oscillated strongly, but dentate did not (Elble *et al.*, 1984). Thus, the dentate could be relatively resistant to tremorogenic oscillation. Most of the cerebellothalamic tract is from dentate, and high-frequency stimulation in this tract is effective for Parkinson's disease and essential tremor. Deep brain stimulation of dentate fibres could disrupt tremorogenic thalamocortical oscillation even if dentate is not the source of oscillation. Our EEG data are consistent with this possibility. The interposed nuclei also project to ventrolateral thalamus, and our EEG data and previous animal studies (Elble *et al.*, 1984) suggest that the interposed nuclei oscillate in essential tremor and Parkinson's disease. Deep brain stimulation of interposed fibres might be necessary for tremor suppression, and excessive stimulation of this pathway could interrupt feedforward motor control (Manto, 2009), explaining the common side effect of ataxia with excessive stimulation (Groppa *et al.*, 2014).

The directions of interactions between the various source signals revealed important differences among Parkinson's tremor, essential tremor and mimicked tremor. Whereas the flow of information at the oscillation frequency is mainly from cerebellum to cerebral cortex in Parkinson's disease and essential tremor, the main direction of interaction is cortico-cerebellar in voluntary movements. This difference probably reflects the greater role of cortical motor planning via the cortico-bulbo-cerebello-thalamo-cortical loop in mimicked tremor. The dentate is known to play an important role in motor planning (Manto, 2009). The mainly cerebello-cortical projection in pathological tremors is consistent with the fact that tremor is an involuntary movement. Cortical motor planning via cerebellum is not needed in pathological tremor, and feedforward motor control by cerebellum, using efferent copies of cortical commands, is more likely to play a role in tremor control than in tremorogenesis (Manto, 2009).

The interactions of cerebral cortex and cerebellum with the muscles also showed clear differences in controls versus patients with Parkinson's disease and essential tremor. In mimicked tremor, the cerebellum mainly received information from the muscles (EMG), and the main projection to the

muscles comes from the primary sensorimotor and premotor cortical regions. This suggests that sensory feedback to cerebellum is necessary to sustain for 2 min the voluntary rhythmic movement in the required frequency range, a task that proved difficult for our healthy controls. In pathological tremors, the oscillatory activity at the tremor frequency was conveyed mainly from cerebellum and from the primary sensorimotor cortex to the muscles. This is consistent with the fact that Parkinson's tremor and essential tremor are involuntary central neurogenic oscillations. Oscillation in the cortico-bulbo-cerebello-thalamo-cortical loop may be affected by sensory feedback, but sensory feedback is not needed for Parkinson's tremor or essential tremor to occur. Activity flow from cerebellum to muscle is most likely via the cerebello-thalamo-corticospinal pathway, not rubrospinal, because the rubrospinal tract is believed to be small in humans, extending only to upper cervical segments (Nathan and Smith, 1982).

In the present study, the thalamic region of the brain was deliberately neglected to circumvent topographic uncertainties due to the methodological constraints of EEG source analysis (Groppa *et al.*, 2013; Sporns, 2013; Papmeyer *et al.*, 2015; Zhan *et al.*, 2017). The large electrode array used in the present study may overcome some of these constraints, but this is not yet clear.

We cannot exclude the possibility that differences in cerebellar source topography reflect differences in the anatomical distribution of tremor, even though we attempted to restrict oscillation to the wrist. However, we believe this is unlikely because our methods searched for cerebral and cerebellar activity that was coherent with the recorded arm muscle. We know from previous studies that tremors in different body segments are not coherent, except in orthostatic tremor (Lauk *et al.*, 1999; Raethjen *et al.*, 2000).

In conclusion, we found a differing topography of cerebellar activity in Parkinson's disease, essential tremor and mimicked tremor. Similar cerebral cortical areas were involved in the two pathological tremors and mimicked tremor, but there was greater cortico-cerebellar and EMG-cerebellar flow in mimicked tremor, consistent with a need for cortical motor planning and continuous sensory feedback in the generation of mimicked tremor. The role of cerebellum in mimicked tremor is undoubtedly the planning and execution of the rhythmic movement. We found only subtle differences between cerebellar involvement in essential tremor versus Parkinson's disease, and their principal role in tremor pathophysiology may be similar, even though there is evidence that oscillation emerges from the basal ganglia in Parkinson's disease (Helmich *et al.*, 2013). Essential tremor is often attributed to the cerebellum, and while the cerebellum is clearly involved in essential tremor, we found no evidence that oscillation emerges from the cerebellum. It may be that the cortico-bulbo-cerebello-thalamo-cortical loop is conducive to oscillation emerging from many areas of the motor system, and the cerebello-thalamo-cortical pathway in particular may promote motor oscillation emerging from any source that connects with this pathway. Neuroimaging methods with increasing spatial and temporal resolution should ultimately identify additional differences among tremor disorders, improving our understanding of tremor pathophysiology.

Acknowledgement

We thank the technical assistant Katrin Lange for her excellent support in recruiting the subjects and doing the EEG recordings.

Funding

This work was supported by the German Research Foundation (DFG; SFB-TR-128, SFB-CRC 1193 and SFB 1261-Project B5). R.E. is also supported by a grant from the Illinois-Eastern Iowa District Kiwanis Neuroscience Foundation.

References

Amjad AM, Halliday DM, Rosenberg JR, Conway BA. An extended difference of coherence test for comparing and combining several independent coherence estimates: theory and application to the study of motor units and physiological tremor. J Neurosci Methods 1997; 73: 69–79.

Benagiano V, Rizzi A, Lorusso L, Flace P, Saccia M, Cagiano R, et al. The functional anatomy of the cerebrocerebellar circuit: a review and new concepts. J Comp Neurol 2018; 526: 769–89.

Broersma M, van der Stouwe AM, Buijink AW, de Jong BM, Groot PF, Speelman JD, et al. Bilateral cerebellar activation in unilaterally challenged essential tremor. Neuroimage Clin 2015; 11: 1–9.

Bucher SF, Seelos KC, Dodel RC, Reiser M, Oertel WH. Activation mapping in essential tremor with functional magnetic resonance imaging. Ann Neurol 1997; 41: 32–40.

Buckner RL, Krienen FM, Castellanos A, Diaz JC, Yeo BT. The organization of the human cerebellum estimated by intrinsic functional connectivity. J Neurophysiol 2011; 106: 2322–45.

Costa J, Gonzalez HA, Valldeoriola F, Gaig C, Tolosa E, Valls-Sole J. Nonlinear dynamic analysis of oscillatory repetitive movements in Parkinson's disease and essential tremor. Mov Disord 2010; 25: 2577–86.

Deuschl G, Bain P, Brin M. Consensus statement of the Movement Disorder Society on Tremor. Ad Hoc Scientific Committee. Mov Disord 1998; 13 (Suppl 3): 2–23.

Dirkx MF, den Ouden HE, Aarts E, Timmer MH, Bloem BR, Toni I, et al. Dopamine controls Parkinson's tremor by inhibiting the cerebellar thalamus. Brain 2017; 140: 721–34.

Elble RJ, Schieber MH, Thach WT Jr. Activity of muscle spindles, motor cortex and cerebellar nuclei during action tremor. Brain Res 1984; 323: 330–4.

Fasano A, Deuschl G. Therapeutic advances in tremor. Mov Disord 2015; 30: 1557–65.

Groppa S, Herzog J, Falk D, Riedel C, Deuschl G, Volkmann J. Physiological and anatomical decomposition of subthalamic neurostimulation effects in essential tremor. Brain 2014; 137 (Pt 1): 109–21.

Groppa S, Muthuraman M, Otto B, Deuschl G, Siebner HR, Raethjen J. Subcortical substrates of TMS induced modulation of the cortico-cortical connectivity. Brain Stimul 2013; 6: 138–46.

Gross J, Ioannides AA. Linear transformations of data space in MEG. Phys Med Biol 1999; 44: 2081–97.

Gross J, Kujala J, Hamalainen M, Timmermann L, Schnitzler A, Salmelin R. Dynamic imaging of coherent sources: studying neural interactions in the human brain. Proc Natl Acad Sci USA 2001; 98: 694–9.

Gross J, Timmermann L, Kujala J, Dirks M, Schmitz F, Salmelin R, et al. The neural basis of intermittent motor control in humans. Proc Natl Acad Sci USA 2002; 99: 2299–302.

Halliday DM, Rosenberg JR, Amjad AM, Breeze P, Conway BA, Farmer SF. A framework for the analysis of mixed time series/point process data–theory and application to the study of physiological tremor, single motor unit discharges and electromyograms. Prog Biophys Mol Biol 1995; 64: 237–78.

Haufe S, Nikulin VV, Muller KR, Nolte G. A critical assessment of connectivity measures for EEG data: a simulation study. Neuroimage 2013; 64: 120–33.

Haykin SS, editor. Kalman filtering and neural networks. New York: Wiley; 2001. pp. 221–69.

Helmich RC, Hallett M, Deuschl G, Toni I, Bloem BR. Cerebral causes and consequences of parkinsonian resting tremor: a tale of two circuits? Brain 2012; 135 (Pt 11): 3206–26.

Helmich RC, Janssen MJ, Oyen WJ, Bloem BR, Toni I. Pallidal dysfunction drives a cerebellothalamic circuit into Parkinson tremor. Ann Neurol 2011; 69: 269–81.

Helmich RC, Toni I, Deuschl G, Bloem BR. The pathophysiology of essential tremor and Parkinson's tremor. Curr Neurol Neurosci Rep 2013; 13: 378.

Hughes AJ, Daniel SE, Kilford L, Lees AJ. Accuracy of clinical diagnosis of idiopathic Parkinson's disease: a clinico-pathological study of 100 cases. J Neurol Neurosurg Psychiatry 1992; 55: 181–4.

Ilinsky IA, Kultas-Ilinsky K. Motor thalamic circuits in primates with emphasis on the area targeted in treatment of movement disorders. Mov Disord 2002; 17 (Suppl 3): S9–14.

Jenkins IH, Bain PG, Colebatch JG, Thompson PD, Findley LJ, Frackowiak RS, et al. A positron emission tomography study of essential tremor: evidence for overactivity of cerebellar connections. Ann Neurol 1993; 34: 82–90.

Journee HL. Demodulation of amplitude modulated noise: a mathematical evaluation of a demodulator for pathological tremor EMG's. IEEE Trans Biomed Eng 2007; 30: 304–8.

Kaminski M, Ding M, Truccolo WA, Bressler SL. Evaluating causal relations in neural systems: granger causality, directed transfer function and statistical assessment of significance. Biol Cybern 2001; 85: 145–57.

Lauk M, Köster B, Timmer J, Guschlbauer B, Deuschl G, Lücking CH. Side-to-side correlation of muscle activity in physiological and pathological human tremors. Clin Neurophysiol 1999; 110: 1774–83.

Mader M, Mader W, Sommerlade L, Timmer J, Schelter B. Block-bootstrapping for noisy data. J Neurosci Methods 2013; 219: 285–91.

Manto M. Mechanisms of human cerebellar dysmetria: experimental evidence and current conceptual bases. J Neuroeng Rehabil 2009; 6: 10.

Maris E, Oostenveld R. Nonparametric statistical testing of EEG- and MEG-data. J Neurosci Methods 2007; 164: 177–90.

Maris E, Schoffelen JM, Fries P. Nonparametric statistical testing of coherence differences. J Neurosci Methods 2007; 163: 161–75.

Mitra PP, Pesaran B. Analysis of dynamic brain imaging data. Biophys J 1999; 76: 691–708.

Moeller F, Muthuraman M, Stephani U, Deuschl G, Raethjen J, Siniatchkin M. Representation and propagation of epileptic activity in absences and generalized photoparoxysmal responses. Hum Brain Mapp 2013; 34: 1896–909.

Muthuraman M, Galka A, Deuschl G, Heute U, Raethjen J. Dynamical correlation of non-stationary signals in time domain–a comparative study. Biomed Signal Process Control 2010a; 5: 205–13.

Muthuraman M, Heute U, Arning K, Anwar AR, Elble R, Deuschl G, et al. Oscillating central motor networks in pathological tremors and voluntary movements. What makes the difference? Neuroimage 2012; 60: 1331–9.

Muthuraman M, Heute U, Deuschl G, Raethjen J. The central oscillatory network of essential tremor. Conf Proc IEEE Eng Med Biol Soc 2010b; 2010: 154–7.

Muthuraman M, Raethjen J, Hellriegel H, Deuschl G, Heute U. Imaging coherent sources of tremor related EEG activity in patients with Parkinson's disease. Conf Proc IEEE Eng Med Biol Soc 2008; 2008: 4716–19.

Nathan PW, Smith MC. The rubrospinal and central tegmental tracts in man. Brain 1982; 105 (Pt 2): 223–69.

Neumaier A, Schneider T. Estimation of parameters and eigenmodes of multivariate autoregressive models. ACM Trans Math Softw 2001; 27: 27–57.

Newman ME. Modularity and community structure in networks. Proc Natl Acad Sci USA 2006; 103: 8577–82.

Papmeyer M, Sussmann JE, Hall J, McKirdy J, Peel A, Macdonald A, et al. Neurocognition in individuals at high familial risk of mood disorders with or without subsequent onset of depression. Psychol Med 2015; 45: 3317–27.

Raethjen J, Lindemann M, Schmaljohann H, Wenzelburger R, Pfister G, Deuschl G. Multiple oscillators are causing parkinsonian and essential tremor. Mov Disord 2000; 15: 84–94.

Rosenberg JR, Amjad AM, Breeze P, Brillinger DR, Halliday DM. The Fourier approach to the identification of functional coupling between neuronal spike trains. Prog Biophys Mol Biol 1989; 53: 1–31.

Salvador R, Suckling J, Coleman MR, Pickard JD, Menon D, Bullmore E. Neurophysiological architecture of functional magnetic resonance images of human brain. Cereb Cortex 2005; 15: 1332–42.

Schneider T, Neumaier A. Algorithm 808: ARfit: a matlab package for the estimation of parameters and eigenmodes of multivariate autoregressive models. ACM Trans Math Softw 2001; 27: 58–65.

Schnitzler A, Munks C, Butz M, Timmermann L, Gross J. Synchronized brain network associated with essential tremor as revealed by magnetoencephalography. Mov Disord 2009; 24: 1629–35.

Sekihara K, Scholz B. Generalized Wiener estimation of three-dimensional current distribution from biomagnetic measurements. IEEE Trans Biomed Eng 1996; 43: 281–91.

Sporns O. Structure and function of complex brain networks. Dialogues Clin Neurosci 2013; 15: 247–62.

Timmermann L, Gross J, Dirks M, Volkmann J, Freund HJ, Schnitzler A. The cerebral oscillatory network of parkinsonian resting tremor. Brain 2003; 126 (Pt 1): 199–212.

van Veen BD, Van Drongelen W, Yuchtman M, Suzuki A. Localization of brain electrical activity via linearly constrained minimum variance spatial filtering. IEEE Trans Biomed Eng 2002; 44: 867–80.

Wan EA, Nelson AT. Dual extended Kalman filter methods. In: Haykin S, editor. Kalman filtering and neural networks. Hoboken, NJ: John Wiley & Sons; 2001. p. 123–73.

Welch P. The use of fast Fourier transform for the estimation of power spectra: a method based on time averaging over short, modified periodograms. IEEE Trans Audio Electroacoustics 1967; 15: 70–3.

Wolters CH, Anwander A, Berti G, Hartmann U. Geometry-adapted hexahedral meshes improve accuracy of finite-element-method-based EEG source analysis. IEEE Trans Biomed Eng 2007; 54: 1446–53.

Zeuner KE, Deuschl G. An update on tremors. Curr Opin Neurol 2012; 25: 475–82.

Zhan L, Jenkins LM, Wolfson O, GadElkarim JJ, Nocito K, Thompson PM, et al. The significance of negative correlations in brain connectivity. J Comp Neurol 2017; 525: 3251–65.